

Many-Spin Interactions and Spin Excitations in Mn_{12}

M. I. Katsnelson

Institute of Metal Physics, Ekaterinburg 620219, Russia

V. V. Dobrovitski and B. N. Harmon

Ames Laboratory, Iowa State University, Ames, Iowa 50011

(March 17, 2018)

In this work, the many-spin interactions taking place in Mn_{12} large-spin clusters are extensively studied using the 8-spin model Hamiltonian, for which we determine the possible parameters based on experimental data. Account of the many-spin excitations satisfactorily explains positions of the neutron scattering peaks, results of EPR measurements and the temperature dependence of magnetic susceptibility. In particular, strong Dzyaloshinsky-Morya interactions are found to be important for description of neutron scattering data. The role of these interactions for the relaxation of the magnetization is qualitatively discussed.

75.40.Mg, 75.10.Dg, 75.50.-y, 75.25.+z

INTRODUCTION

In the last years, a new kind of magnetic compounds, the magnetic molecules, has been drawing the attention of physicists as well as chemists¹. Such molecules each contain a large number (typically, 10 to 20) of paramagnetic ions (such as Mn, Fe or Cu) coupled by exchange interactions. Each molecule, therefore, presents a mesoscopic system that is neither totally microscopic, nor totally macroscopic, but where micro- and macroscopic behavior coexist. These materials are promising for various practical applications². On the other hand, the coexistence of quantum and classical behavior in the clusters makes them very suitable objects for study of macroscopic quantum effects in spin systems^{3,4}. These studies, clarifying many problems of quantum theory of measurements⁵, are also important for development of a physical basis for practical implementation of powerful algorithms of quantum computations, quantum cryptography and quantum searching⁶.

Particularly, the $\text{Mn}_{12}\text{O}_{12}(\text{CH}_3\text{COO})_{16}(\text{H}_2\text{O})_4$ molecules (below referred to as Mn_{12}) recently became a subject of great interest. Each molecule^{7,8} contains a cluster of twelve manganese ions surrounded by acetate radicals and water molecules. The ground state of the clusters corresponds to a large total spin $S = 10$. The clusters possess a strong easy-axis anisotropy: the zero-field splitting between the states with $S_z = \pm 10$ and $S_z = \pm 9$ (where S_z is the value of z -projection of the total cluster spin) is 14.4 K. Being stacked into a crystal, the molecules form a tetragonal lattice; in so doing the magnetic interactions between different clusters are very small (of order

of 10^{-2} T). Thus, the crystal consisting of these molecules can be considered as an assembly of ideal noninteracting superparamagnetic entities, each being identical to the others.

These clusters have been successfully used for the study of mesoscopic quantum effects. In particular, resonant magnetization tunneling has been unambiguously registered in experiments on Mn_{12} ^{9,10}. Moreover, there are experimental results^{12,13} supporting the hypothesis of "ground state-to-ground state" tunneling in Mn_{12} below 2 K (for more detailed discussion, see Sec. VI).

However, the progress in understanding the physical properties of Mn_{12} is greatly hampered by the lack of an adequate description of these clusters. Indeed, the description of Mn_{12} as a single spin $S = 10$ entity has been the starting point in most works devoted to this subject. We know of only a few theoretical attempts to account for the internal spin structure of the cluster^{8,14,15}, but even in these the relativistic anisotropic interactions have not been taken into account. In view of recent experiments^{16,17,18} showing that the single-spin model is seriously deficient, it is worthwhile reconsidering the many-spin aspects of Mn_{12} .

In this paper we focus on the many-spin interactions in Mn_{12} clusters. We account for not only isotropic exchange interactions between ions in the cluster, but also various anisotropic interactions possibly present in Mn_{12} . Based on the results, we propose a spin Hamiltonian for these clusters. We show that this Hamiltonian can reproduce satisfactorily most recent experimental results, such as positions of neutron scattering peaks, high-frequency EPR data and the experimental dependence of the magnetic susceptibility on temperature. We note that the account of anisotropic interactions, especially the Dzyaloshinsky-Morya interaction (which has been missing up to now), is crucial for a detailed description of the experimental data.

The paper is organized as follows. In Sec. I we describe the basic model of Mn_{12} used in this work and establish roughly its domain of validity. In Sec. II we derive and discuss the spin Hamiltonian for this model. Sec. III is devoted to discussion of relevant experimental data. In Sec. IV the numerical procedure used for calculations is discussed and the possible parameters of the spin Hamiltonian are presented. Comparison with experimental data is made. The results obtained are analyzed qualitatively and discussed in Sec. V, where the interpretation

of the neutron scattering data is presented. In Sec. VI we qualitatively discuss the relation between Dzyaloshinsky-Morya interactions and magnetic relaxation in Mn_{12} . A summary is provided in Sec. VII.

I. THE DIMERIZED 8-SPIN MODEL OF Mn_{12}

The cluster Mn_{12} , schematically shown in Fig. 1, consists of eight Mn^{3+} ions having the spin 2 and four Mn^{4+} ions having the spin $3/2$. The ions are coupled by exchange interactions, indicated in Fig. 1 by different lines connecting the ions. The values of the exchange integrals are not known, but estimates are given in Ref. 8: $J_1 = -150 \text{ cm}^{-1}$ (AFM exchange), $J_2 = J_3 = -60 \text{ cm}^{-1}$ and $|J_4| < 30 \text{ cm}^{-1}$. These values are rough, but describe correctly the scale of exchange interactions in Mn_{12} . Recent experiments^{16,17,18} show that the excitations with spin values $S < 10$ are rather close to the ground state: the distance is 40–60 K (values differ in different reports). This is less than the energy of some states with the spin $S = 10$ (namely, the states $S_z = 0, \pm 1, \pm 2, \pm 3$), i.e. the lower states of the manifold $S = 9$ are lower than the higher states of the manifold $S = 10$. Thus, an adequate description of Mn_{12} should account for the excitations with $S < 10$; i.e. the cluster should be considered as a many-spin system.

The total number of spin states in Mn_{12} is large even for modern computers. But we can employ the fact that the exchange antiferromagnetic interactions J_1 (see Fig. 1) are much larger than all the others⁸, so corresponding pairs of ions Mn^{3+} and Mn^{4+} form dimers with the total spin $s = 1/2$ (one of this pairs is designated in Fig. 1, it includes ions C and D). This model has already been successfully used for description of spin states of the cluster^{8,15}. Its validity is proven by megagauss-field experiments¹⁹: the states of dimers with the spin s higher than $1/2$ (excitations of dimers) come into play when the external magnetic field is about 400 T, i.e. the excitations of dimers have energy about 370 cm^{-1} . Analogously, the dependence of the magnetic susceptibility of the cluster versus temperature^{4,7,8} shows that the dimer excitations contribute when temperature becomes as high as 150–200 K.

Based on these data, we can analyze the domain of validity of the "dimerized" model. To do this, we note that the exchange interactions J_2 , J_3 and J_4 mix the ground state of a dimer with the dimer excitations, and the approximation of spin- $1/2$ dimers corresponds to the zeroth order perturbation theory with $1/J_1$ as an expansion parameter (similar approach has been used in Ref. 15).

To clarify this point, let us consider the level a having, to the zeroth order, the energy E_a with respect to the ground state. Let us denote the distance between the ground state and the excitation of dimer as $E_{ex} \sim 370 \text{ cm}^{-1}$. The first-order correction to the energy of the

level a is of the order of $J'^2/(E_{ex} - E_a)$, where J' is the magnitude of exchange interactions between dimers and nondimerized spins (see below). Thus, accounting for the first-order corrections, the distance between the ground state and the level a becomes

$$E'_a = E_a + C_a J'^2 [1/(E_{ex} - E_a) - 1/E_{ex}],$$

where C_a is a factor of order of unity, depending on the specific level a . As will be shown below, J' is of order of 70 cm^{-1} ; so the first-order correction for the levels with energies about 70 cm^{-1} is already considerable, of order of 4 cm^{-1} . This estimate, though being rough, gives the correct order of magnitude of the error introduced by the dimerized 8-spin model.

Moreover, this error restricts the region of temperatures where the dimerized model can be successfully applied. E.g., as our calculations show, to obtain the correct value of the magnetic susceptibility χ at the temperature T , we need to account for the levels with energies about $4\text{--}5 kT$. Obviously, the error in positions of these levels will introduce corresponding error in the dependence $\chi(T)$. Its analytical evaluation is difficult, and the comparison of the results of calculations with the experimental data, performed in Sec. IV is the better way to understand the temperature domain of validity of the dimerized model. As our results show, the dimerized model gives reasonable results for temperatures lower than about 50 K.

Recalling that the temperatures below 30 K are of most interest, we conclude that the dimerized model is satisfactory for present needs of experimentalists.

II. THE SPIN HAMILTONIAN OF Mn_{12}

Thus, we consider the Mn_{12} cluster as consisting of four "small" dimer spins $s = 1/2$ and four "large" spins $S = 2$ (corresponding to the four non-dimerized ions Mn^{3+}), coupled by exchange interactions (see Fig. 2). Moreover, we have to account for the anisotropic relativistic interactions in the cluster, so the Hamiltonian of the system can be written as:

$$\mathcal{H} = -J \left(\sum_i \mathbf{s}_i \right)^2 - J' \sum_{\langle k,l \rangle} \mathbf{s}_k \mathbf{S}_l + H_{\text{rel}}, \quad (1)$$

where \mathbf{s}_i are the spin operators of small dimer spins $s = 1/2$, \mathbf{S}_l are spin operators of large spins $S = 2$, and H_{rel} denotes the part of the Hamiltonian describing relativistic interactions in the cluster. Summation in (1) is over pairs of spins coupled by exchange interactions. In the first term of the Hamiltonian we took into account that each small dimer spin is coupled with all the other small spins, so $2 \sum \mathbf{s}_i \mathbf{s}_j = (\sum \mathbf{s}_i)^2$ up to an insufficient additive constant.

To zeroth order in J_1 , the exchange integrals of the dimerized models are connected with the initial exchange parameters J_2 , J_3 and J_4 as follows:

$$J = -J_2/2, \quad J' = -J_3 + 2J_4. \quad (2)$$

Since the values of J_2 , J_3 and J_4 are not known, the parameters J and J' are to be determined from experimental data (see Sec. IV).

Furthermore, different types of relativistic anisotropic magnetic interactions possibly present in Mn_{12} clusters should be included in the Hamiltonian. A large easy-axis anisotropy in the cluster is one of most important features to be taken into account. Generally, this anisotropy arises due to the single-site anisotropy of large spins (spins of Mn^{3+} ions) and various kinds of anisotropic exchange. We performed calculations for three basic types of easy-axis anisotropy in the cluster:

$$H_{\text{rel}}^1 = -K_z \sum_{i=1}^4 (S_i^z)^2, \quad (3a)$$

$$H_{\text{rel}}^2 = -J_{zz} \sum_{\langle i,j \rangle} s_i^z s_j^z, \quad (3b)$$

$$H_{\text{rel}}^3 = -J_{zz} \sum_{\langle i,j \rangle} s_i^z s_j^z, \quad (3c)$$

where summations in (3b) and (3c) are over exchange-coupled pairs of spins. Anisotropy parameters (K_z , J_{zz} or J_{zz}) have been chosen to give a correct value of the zero-field splitting between the states $S_z = \pm 10$ and $S_z = \pm 9$ (14.4 K). All three types of anisotropy give rather close energies of low-lying excitations (of energy less than 40 K), but higher excitations are reproduced best if the anisotropy is assumed to be of single-site type (3a), so we can conclude that the easy-axis anisotropy is primarily of single-site type. This result agrees with the conclusion drawn in Ref. 21. We will consider only this kind of anisotropy.

Another potentially important sort of relativistic interaction is an in-plane anisotropy of large spins, i.e. H_{rel} can include a contribution of the form:

$$H_{\text{rel}}^4 = K_1 \left[(S_1^x)^2 + (S_2^y)^2 + (S_3^x)^2 + (S_4^y)^2 \right], \quad (4)$$

where the presence of fourth-order symmetry axis in the cluster is directly taken into account. The small spins $s = 1/2$ are excluded since $(\sigma_x)^2 = (\sigma_y)^2 = (\sigma_z)^2 = 1$ for Pauli matrices σ_x , σ_y and σ_z ; and only spins of non-dimerized Mn^{3+} ions give a nontrivial contribution. These ions are surrounded by eight oxygen ions forming a distorted octahedron. The axes of oxygen octahedra are significantly tilted from the c -axis of the cluster, therefore, this term can be relatively large, even comparable to the easy-axis anisotropy. But, surprisingly, our results show that this kind of interaction gives negligible effect, except for trivial renormalization of the easy-axis anisotropy constant K_z in (3a). If we account for this renormalization, the positions and the wave functions of excited levels remain almost unaffected even for $K_1 = 3K_z$ (i.e., for the in-plane anisotropy three times

larger than the easy-axis one). Thus, this kind of interaction can be excluded from further considerations.

Another important interaction is Dzyaloshinsky-Morya (DM) antisymmetric exchange. To our knowledge, the possible presence of DM-interactions in Mn_{12} was first suggested in Ref. 18, but little attention has been paid until now. Our results show that these interactions are, indeed, very important and have rather large magnitude.

A pair of ions coupled by DM-interaction is described by the Hamiltonian

$$H_{\text{DM}} = \mathbf{D} \cdot [\mathbf{S}_1 \times \mathbf{S}_2], \quad (5)$$

and the magnitude of the DM-vector \mathbf{D} can be estimated as²² $D \sim \lambda A$, where A is the isotropic (nonrelativistic) exchange coupling between ions and λ is the spin-orbit coupling constant (which is rather small for transition ions). For comparison, the magnitude of easy-axis anisotropy is estimated as $K_z \sim \lambda^2 A$, i.e. is of next order of smallness in comparison with D . Thus, the DM-interactions in Mn_{12} can be expected to be important.

In the 8-spin model of the cluster there are DM-interactions of two kinds:

$$H_{\text{DM}} = \sum_{\langle i,j \rangle} \mathbf{D}^{i,j} \cdot [\mathbf{s}_i \times \mathbf{s}_j] \quad (6a)$$

$$H_{\text{DM}}^1 = \sum_i \sum_j \mathbf{D}_1^{i,j} \cdot [\mathbf{s}_i \times \mathbf{s}_j]. \quad (6b)$$

Summation in (6a) is over exchange-coupled pairs of spins; summation in (6b) is over all pairs of dimer spins, since all dimer spins interact with each other. We studied both kinds of DM-interaction and found that the second kind, i.e. H_{DM}^1 involving small spins can be neglected. Therefore, we can neglect the interactions of the type (6b).

The crystal field in Mn_{12} , governing the DM-interactions, possesses certain symmetry elements, thus imposing restrictions on the values of $\mathbf{D}^{i,j}$. It is reasonable (and rather standard²²) to assume that the crystal field is determined mainly by the oxygen octahedra surrounding manganese ions in the cluster; so the symmetry of the crystal field is governed by the mutual arrangement of the oxygen octahedra. The following two symmetry elements are of interest for us. The first one is the fourth-order rotary-reflection axis^{7,8} parallel to the c -axis of the cluster. This symmetry is obviously preserved in the 8-spin model of the cluster, so the two DM-vectors $\mathbf{D}^{1,5}$ and $\mathbf{D}^{1,8}$ (see Fig. 2) define all the other $\mathbf{D}^{i,j}$. The other element of symmetry is the mirror plane ρ parallel to the z -axis passing through the ions C and D (see Fig. 1). The oxygen octahedra surrounding the ions A and B (see Fig. 1) are invariant with a good degree of accuracy²⁰ with respect to reflection in the plane ρ (inspection of the structure data supplied in Refs. 7, 8 shows this); this symmetry is also preserved in the 8-spin model. Thus, the vector $\mathbf{D}^{1,8}$ (Fig. 2) defines all the other DM-vectors in the Hamiltonian (6a):

$$D_x^{1,8} = -D_x^{1,5} = D_y^{2,5} = -D_y^{2,6} = -D_x^{3,6} = D_x^{3,7} \quad (7a)$$

$$= -D_y^{4,7} = D_y^{4,8},$$

$$D_y^{1,8} = D_y^{1,5} = -D_x^{2,5} = -D_x^{2,6} = -D_y^{3,6} = -D_y^{3,7} \quad (7b)$$

$$= D_x^{4,7} = D_x^{4,8},$$

$$D_z^{1,8} = -D_z^{1,5} = D_z^{2,5} = -D_z^{2,6} = D_z^{3,6} = -D_z^{3,7} \quad (7c)$$

$$= D_z^{4,7} = -D_z^{4,8}.$$

Obviously, any other vector $\mathbf{D}^{i,j}$ can be taken as a basis instead of $\mathbf{D}^{1,8}$. No other symmetry elements allow for further reduction, so DM-interactions in Mn_{12} are described using three parameters: $D_x^{1,8}$, $D_y^{1,8}$ and $D_z^{1,8}$. Below, these parameters are denoted simply as D_x , D_y and D_z .

As our results show, in the DM-Hamiltonian (6a) the terms proportional to D_y produces negligible matrix elements (a few percent in comparison with other terms). It occurs due to symmetry reasons: the inspection of the relations (7) shows that the components D_x and D_z transform antisymmetrically with respect to reflection in the plane ρ , but the component D_y transforms symmetrically. The matrix elements of the terms proportional to D_y nearly cancel each other, leading to negligible matrix elements. Therefore, these terms are excluded from consideration and we set $D_y = 0$ with negligible error.

Finally, having studied all the interactions described above, we can write down the Hamiltonian of the cluster in the following form:

$$\mathcal{H} = -J \left(\sum_i \mathbf{s}_i \right)^2 - J' \sum_{\langle k,l \rangle} \mathbf{s}_k \mathbf{s}_l - K_z \sum_{i=1}^4 (S_i^z)^2 \quad (8)$$

$$+ \sum_{\langle i,j \rangle} \mathbf{D}^{i,j} \cdot [\mathbf{s}_i \times \mathbf{s}_j],$$

where the DM-vectors $\mathbf{D}^{i,j}$ obey the relations (7) with the parameter $D_y^{1,8} \equiv D_y = 0$.

III. REVIEW OF RELEVANT EXPERIMENTAL RESULTS

At present, data of various experiments on magnetic molecules Mn_{12}Ac are available, including the temperature dependence of the effective magnetic moment of the cluster $\mu_{\text{eff}}(T)^{7,8,16}$, the results of EPR experiments^{21,23}, dynamic susceptibility measurements²⁴, inelastic neutron scattering data¹⁶ and specific heat data¹⁷. Unfortunately, only few of these data can be used for determining the parameters of the 8-spin Hamiltonian for Mn_{12} clusters.

Recent high-frequency EPR experiments²¹ refined the description of the easy-axis anisotropy of the cluster and showed that the anisotropy Hamiltonian in the single-spin model can be approximated as follows:

$$H = \alpha \mathcal{S}_z^2 + \beta \mathcal{S}_z^4 + \gamma (\mathcal{S}_+^4 + \mathcal{S}_-^4), \quad (9)$$

$$\alpha = -0.56 \text{ K}, \quad \beta = -11.08 \cdot 10^{-4} \text{ K},$$

$$\gamma = 2.88 \cdot 10^{-5} \text{ K},$$

where \mathcal{S}_z , \mathcal{S}_+ and \mathcal{S}_- denote the operators of the total spin of the cluster. It means, in terms of a many-spin approach, that the energies of the low-lying levels with spin $\mathcal{S} = 10$ obey Eq. (9). It is worth noting that the derived values of quartic corrections β and γ are rather large and, as our calculations show (see below), seem to be poorly explained using the single-spin description of Mn_{12} , i.e. when accounting only for the states belonging to the $\mathcal{S} = 10$ manifold. Our results show that the excited levels with $\mathcal{S} < 10$ are necessary to give reasonable values for the quartic corrections.

Another set of results, very useful for elucidating the many-spin interactions in Mn_{12}Ac , is the neutron scattering results supplied in Ref. 16. The experiments have been performed at very low temperatures (mostly, 1.5 K to 2.5 K), where only the lowest levels $\mathcal{S}_z = \pm 10$ are populated. Since the selection rule for neutron scattering is $\delta \mathcal{S}_z = 0, \pm 1$, only the levels with $\mathcal{S}_z = \pm 9$ can give rise to scattering peaks (the levels with $\mathcal{S}_z = \pm 11$ have too large energies¹⁹ and can be excluded).

Results of these experiments can be summarized as follows. A prominent peak of spin origin at about 0.3 THz has been detected and attributed to the transitions to the levels with $\mathcal{S} = 10$, $\mathcal{S}_z = \pm 9$, in excellent agreement with all previous data (0.3 THz corresponds to about 14.4 K). At higher energies, two sets of peaks have been detected around 1.2 THz and 2.0 THz. The fitting proposed in Ref. 16 gives two peaks in the first set (at energies about 57 K and 66 K) and three peaks in the second set (at energies 90 K, 96 K and 105 K); but authors indicate clearly that possibly more peaks are present (most likely, three peaks in the first set and four or five in the second). Another interesting detail of the neutron scattering spectra is a very broad mode situated at about 0.2 THz; this mode disappears when the temperature is less than about 2 K.

The authors have not managed to interpret these features, except for the peak at 0.3 THz. They pointed out that there is particular difficulty in interpretation of the peaks at 1.2–1.3 THz: the model they used for susceptibility fitting gives two degenerate levels $\mathcal{S} = 9$ at about 33 K, an obvious contradiction with the neutron scattering spectrum. We show below that the 8-spin model developed here can overcome these difficulties and gives correct positions for neutrons peaks at 1.2 THz along with a correct description of the susceptibility data.

Thus, we found the following experimental results to be relevant for the purpose of a quantitative description of the Mn_{12} clusters. The distance between the ground state and the first excited level(s) is 14.4 K. The energies (the anisotropy splittings) of the low-lying levels, belonging to the $\mathcal{S} = 10$ manifold, obey formula (9). There are two or three neutron peaks around 60–70 K, two of them are situated at 57 K and 66 K. Also, there are up to five peaks around 100 K, three of them are at 90 K, 96 K and

105 K. The temperature dependence of the susceptibility (or, equivalently, the dependence $\mu_{\text{eff}}(T)$) has the form displayed in Refs. 7, 8, 16 and Fig. 4.

The other experimental results, though providing important information about Mn_{12} , are much less suitable for our purposes (to a large extent, because different, *a priori* equally probable, interpretations are possible).

IV. NUMERICAL CALCULATIONS AND PARAMETERS OF THE 8-SPIN MODEL. COMPARISON WITH EXPERIMENT

Having derived the spin Hamiltonian for the 8-spin model of Mn_{12} , we attempted to extract its parameters from the relevant experimental data.

We used the following two-step numerical scheme. At the first step, the relativistic term H_{rel} has been neglected resulting in an isotropic exchange Hamiltonian. The eigenstates of this Hamiltonian are degenerate with respect to \mathcal{S}_z . Thus, it is sufficient to take into account only the states with $\mathcal{S}_z = 0$, so the exchange Hamiltonian (represented by a matrix 1286×1286) has been diagonalized within the subspace spanned by these states. Then, at the second step, the relativistic anisotropic interactions have been taken into account. Among the states obtained at the first step (having $\mathcal{S}_z = 0$), we retain only those with the energy less than E_{cut} (a sufficiently large value for this parameter has been chosen) and generate the corresponding states with different \mathcal{S}_z (basis states). Then the complete Hamiltonian (8) has been diagonalized within the subspace spanned by the generated basis states. Calculations with different values of E_{cut} have been performed to assure that the positions of lower levels are obtained with desired accuracy. Typical values of E_{cut} were about 250 K: the levels with higher energies are not worth including due to the limited accuracy of the 8-model itself (see Sec. I).

Based on the procedure described above, the fitting of relevant experimental data (Sec. III) has been made and the possible parameters of the 8-spin Hamiltonian determined.

Neutron scattering data are of primary interest for us. We focus our attention on the positions of the neutron peaks, since the amplitudes depend strongly on details of the experiments. We first assume an ideal experiment, where the resolution of the setup is infinite and the neutrons with all possible scattering vectors are detected (i.e., the detector has infinite aperture). In this case, at zero temperature, the cross-section of neutron scattering at the energy E is^{16,25}

$$\sigma(E) = \int_{\mathbf{R}^3} d^3\mathbf{q} A F^2(q) \sum_{a,b} (\delta_{a,b} - q_a q_b / q^2) \times \sum_{m,n} \exp[i\mathbf{q}(\mathbf{r}_m - \mathbf{r}_n)] \quad (10)$$

$$\times \sum_{\psi} \langle 0 | S_m^a | \psi \rangle \langle \psi | S_n^b | 0 \rangle \delta(E(\psi) - E),$$

where A is a constant, $F(q)$ is the form-factor of manganese ions, \mathbf{q} is a scattering vector, n, m enumerate different ions, and a, b refer to the Cartesian coordinates (x, y and z). The integration is performed over all vectors \mathbf{q} . $E(\psi)$ denotes the energy of the state ψ , $|0\rangle$ denotes the ground state, which is the only one populated at zero temperature. The transitions with $\Delta\mathcal{S}_z = 0, +1$ can be neglected since there is only one state $\mathcal{S}_z = 10$ and no states $\mathcal{S}_z = 11$. In this case, the total cross-section (10) is proportional to the quantity

$$V = \sum_i \left| \langle \phi_i^{(9)} | \psi \rangle \right|^2, \quad (11)$$

where the state ψ has the energy $E(\psi) = E$ with respect to the groundstate; i.e., the state ψ is the final state of the neutron scattering process and gives rise to a neutron peak at the energy $E(\psi)$ of the amplitude proportional to V . The summation in (11) is performed over all basis levels having $\mathcal{S}_z = 9$; these levels are denoted as $\phi_i^{(9)}$. Equation (11) expresses the simple fact that only the transitions with $\Delta\mathcal{S}_z = -1$ are allowed in the neutron scattering process, since the transitions with $\Delta\mathcal{S}_z = 0, +1$ are absent. Below, the quantity V is referred to as a normalized cross-section for the level ψ . Our results show that V discriminates easily the eigenstates which can give rise to noticeable neutron scattering peaks.

Furthermore, the values of parameters α and β describing the easy-axis anisotropy in Eq. (9), have been taken into account in determination of the cluster parameters. The energies of the five lowest levels, having spin $\mathcal{S} = 10$, have been approximated by a fourth-order polynomial, following Eq. (9), and the coefficients α and β have been extracted and compared to the experimental data.

As a result of calculations, the following three sets of the cluster parameters have been found to provide the best fitting of experimental data:

Set A: $J = 0$, $J' = 105$ K, $K_z = 5.69$ K, $D_z = -1.2$ K, $D_x = 25$ K;

Set B: $J = 23.8$ K, $J' = 79.2$ K, $K_z = 5.72$ K, $D_z = 10$ K, $D_x = 22$ K;

Set C: $J = 41.4$ K, $J' = 69$ K, $K_z = 5.75$ K, $D_z = 10$ K, $D_x = 20$ K.

The positions of neutron peaks calculated for these sets of parameters are presented in Fig. 3. The graphs show the dependence of normalized cross-section vs. the level energy. It is seen from these figures, that the normalized cross-section is extremely small (less than 10^{-2}) for most of levels, and only few states can give rise to noticeable neutron scattering peaks. Moreover, to facilitate

the analysis of the data for reader, the positions of neutron peaks are listed in the Table I. The values of the easy-axis anisotropy parameters α and β are listed in the Table II.

As the results show, each of the parameter sets reproduces reasonably well its own portion of the experimental results. All the sets give reasonably good positions of the low-energy neutron peaks at 0.3 THz (14.4 K), 1.19 THz (57 K) and 1.38 THz (66 K). The parameter set A also gives the values of anisotropy parameters α and β , rather close to the experimental ones, but the neutron peaks corresponding to higher energies (around 2 THz) are reproduced poorly. The parameter sets B and C give correctly only the order of magnitude of α and β , but reproduce better the positions of the high-energy neutron peaks.

Finally, the temperature dependence of the effective magnetic moment μ_{eff} of the cluster has been calculated for all three sets of parameters using the formula

$$\mu_{\text{eff}}(T) \equiv \sqrt{3\chi(T) \cdot kT}, \quad (12)$$

where χ is the susceptibility of the cluster, k is Boltzmann's constant and T is the temperature. The susceptibility $\chi(T)$ has been calculated in a way reproducing the experimental procedure. The Zeeman term, describing the effect of an external field has been introduced into the Hamiltonian (8). The field magnitude $H = 1$ mT has been chosen following Ref. 16. The resulting Hamiltonian has been diagonalized, and the component of the cluster spin S_H along the field has been calculated by means of quantum-statistical averaging over the Gibbs canonical ensemble. This routine has been repeated several times for different orientations of the field, and the obtained values of S_H have been averaged. It corresponds to a powder sample measurements, when the crystallites are randomly oriented with respect to the field. The susceptibility χ , following a standard experimental procedure, has been calculated as a ratio of the resulting average cluster spin to the field magnitude H . Finally, the value μ_{eff} has been obtained applying Eq. (12).

The curves μ_{eff} calculated for the three sets of cluster parameters, are presented in Fig. 4 along with the experimental data. All the sets give almost coinciding curves, and below 50 K the agreement with experiment is good. The region of temperatures higher than 50 K can not be reproduced satisfactorily: as our test calculations showed, to obtain the correct value of effective moment μ_{eff} at the temperature T , we need to account for the levels with energies about $4\text{--}5kT$. When calculating the curves presented, only the levels with energies less than 250 K have been taken into account, thus restricting the correctly described temperature region.

V. QUALITATIVE ANALYSIS OF THE RESULTS AND INTERPRETATION OF EXPERIMENTAL DATA

At present, having rather limited number of the relevant experimental data, it is hard to distinguish between the parameter sets A, B and C. The easy-axis anisotropy parameters α and β are obtained with good precision in EPR experiments, but the magnetization measurement data¹⁸ suggest other values for these parameters; so, comparison of the experimental values of α and β with our results can not serve as a definitive basis for judgement. Also, the quality of the description of the high-energy neutron peaks can not be decisive, since the disagreement can be attributed to the limited accuracy of the dimerized 8-spin model itself. Megagauss-field experiments¹⁹, along with careful measurements of the low-energy peaks (around 1.2 THz) and fitting of their amplitudes seems to be a promising strategy for future investigations.

Nevertheless, the results already obtained provide new important information about the role of many-spin interactions in Mn_{12} clusters. In this section we focus our attention on the qualitative consideration of the results obtained and discuss the interpretation of the experimental data.

First, it is worthwhile to note that the consideration of states with spin S less than 10 leads to rather large quartic corrections to the energy of easy-axis anisotropy. If these excited states are not taken into account, i.e. if only the states with $S = 10$ are included, the value of β is of order of 10^{-5} K.

Another important fact is the large magnitude of the Dzyaloshinski-Morya (DM) interactions in the cluster Mn_{12} . In our opinion, this can be attributed to the low symmetry of the cluster. Indeed, the strength of the DM-interaction is governed to a large extent by asymmetry of crystal field acting on the interacting ions²². An instructive example is provided in Ref. 26: the DM-interaction can emerge for ions located at the surface of a magnet, even though these interactions are prohibited for ions in the bulk of the magnet. In some sense the Mn_{12} molecule possesses "surface" everywhere, and the symmetry of the crystal field is rather low.

The presence of the large Dzyaloshinsky-Morya term in the Hamiltonian provides a key to an explanation of the neutron scattering data. First, the DM-terms lead to the appearance of the two neutron peaks around 1.2 THz. If these terms are absent, there are two degenerate levels with $S_z = 9$ around 1.2 THz. Among all the interactions we considered (see Sec. II), only the DM-interaction can lift this degeneracy and provide a large splitting (about 9 K), as observed in experiments. Similarly, according to our calculations, several peaks around 2 THz appear only due to DM-interactions.

The origin of the peak at 0.3 THz has been completely explained in Ref. 16: it appears because of easy-axis anisotropy splitting the levels with different S_z . Our re-

sults agree with this conclusion.

An interesting feature in the neutron scattering data is the broad mode situated at 0.2 THz. No states of this energy have been observed, e.g., in EPR-experiments^{8,21,23}. Our calculations also show no states with the energy 0.2 THz (or, equivalently, about 10 K). In our opinion, this mode is caused by an interaction of Mn₁₂ clusters with the dissipative environment. Due to this interaction, each level broadens (nonuniform broadening), forming a quasiband of finite width δE (see Refs. 11, 27 for details). The value of $\delta E \approx 2$ K can be estimated from the single-crystal hysteresis measurements¹⁰. Transitions between the two quasibands take place, so, along with the peak at 0.3 THz (14.4 K), a broad mode of inter-quasiband transitions appears. It happens when different states in the quasibands are populated, i.e. at the temperatures of order of $\delta E \approx 2$ K, which agrees with experiment. Energies of the inter-quasiband transitions are reduced by the value about $2 \cdot \delta E \approx 4$ K, so the corresponding neutron scattering mode is situated around $E_b = 14.4 \text{ K} - 2 \cdot \delta E \approx 10.4 \text{ K}$, or, equivalently, around 0.2 THz, in agreement with experiment. At increasing temperatures, the occupancy of quasibands becomes more uniform, so the intensity of the broad mode increases along with the decrease in intensity of the peak at 14.4 K. This behavior also agrees with experiment. However, this qualitative explanation can not be considered as sufficient, and a rigorous quantitative treatment is necessary. Such a treatment constitutes a separate physical problem to be investigated in the future.

VI. DZIALOSHINSKY-MORYA INTERACTIONS AND THE RELAXATION OF MAGNETIZATION

Strong Dzyaloshinsky-Morya interactions can play an important role in relaxation of magnetization in Mn₁₂ clusters. The possible importance of DM-interactions for the relaxational properties of Mn₁₂ was already mentioned in Ref. 18, but no analysis was made. Below, the relation between the DM-interaction and relaxation is analyzed qualitatively.

The relaxation time in Mn₁₂ is very long, about 2 months at 2 K. At relatively high temperatures the magnetization relaxation time τ follows the Arrhenius law $\tau = \tau_0 \exp(-\Delta E/kT)$ with $\tau_0 = 2.4 \cdot 10^{-7}$ sec and the effective barrier $\Delta E = 61 \text{ K}^8$. At low temperatures the situation changes: the experimental results presented in Refs. 12, 13 show that τ saturates below the crossover temperature $T_c = 2 \text{ K}$, which is attributed to the onset of "ground state - to - ground state" tunneling. Such a high value of the crossover temperature poses certain problems, since at present the nature of magnetic relaxation in Mn₁₂ is unknown. Important information has been supplied by hysteresis measurements^{9,10}: it has been directly shown that the relaxational mechanism in Mn₁₂ should allow for transitions between the states $|\mathcal{S}_z\rangle$ and $|\mathcal{S}_z \pm 1\rangle$.

The relaxation of magnetization has been extensively studied^{28,29,30} within the single-spin model of Mn₁₂. The Hamiltonian (9) of this model provides transitions with $\Delta \mathcal{S}_z = \pm 4$ only, and an external transversal field H_x is necessary to allow the $\Delta \mathcal{S}_z = \pm 1$ transitions. Different sources of this field have been considered: a hyperfine field induced by nuclear spins²⁸ and a dipole-dipole field induced by other clusters³⁰. There are certain difficulties facing these interpretations. E.g., as reported in Refs. 11, 31, the relaxation rate increases on dilution of Mn₁₂ in solution, although the dipole-dipole interactions between the clusters decreases; this seems to be difficult to explain with the relaxation mechanism based on intercluster dipole-dipole interactions³⁰. The other mechanism, based on the hyperfine fields²⁸ can not easily explain the high value of the crossover temperature.

Strong Dzyaloshinsky-Morya interactions constitute another source of magnetic relaxation in Mn₁₂. It obviously allows the $\Delta \mathcal{S}_z = \pm 1$ transitions. On solution, the dipole-dipole fluctuating fields between the clusters decrease, thus decreasing the decohering influence of the environment, so the relaxation rate increases. This agrees with experimental results¹¹. Relatively large magnitude of DM-interactions can, in principle, explain the high value (2 K) of the crossover temperature. This shows that the quantitative study of DM-based relaxation in Mn₁₂ is important.

Nevertheless, we emphasize that, to our knowledge, current information is not sufficient for judgement in favor of some single relaxation mechanism. At present, all of them can be considered as equally probable, and the possibility of a combination of different mechanism exists.

Independent of the problem of relaxation in Mn₁₂, DM-interactions present an interesting and important mechanism for magnetic relaxation. It can be significant, for example, in nanosized particles, where large DM-interactions can arise due to reduced symmetry at the surface²⁶. The relaxation based on this interaction is rather unusual: it is related not to the potential barrier created by easy-axis anisotropy, but to the barrier created by isotropic exchange. The point is that the Dzyaloshinsky-Morya term H_{DM} couples the states with different values of total spin \mathcal{S} , i.e.

$$\langle \mathcal{S}, \mathcal{S}_z | H_{\text{DM}} | \mathcal{S} \pm 1, \mathcal{S}_z \pm 1 \rangle \neq 0. \quad (13)$$

This feature differs drastically from standard consideration of relaxation in small particles, where only the anisotropy barrier is usually taken into consideration.

Isotropic exchange interactions are usually rather strong, but it does not necessarily means that the DM-based relaxation is negligible. E.g., in spin-frustrated systems the height of the exchange barrier can be considerably reduced. Moreover, it can be significant in certain non-frustrated systems. For the relaxation based on DM-interactions, the relaxation time should be governed by the ratio D/A , where D is the absolute value of

Dzyaloshinsky-Morya vector and A is the exchange integral. On the other hand, for "conventional" relaxation mechanism, when the anisotropy barrier is overcome, the ratio U/K governs the relaxation rate, where K is the anisotropy constant and U is the strength of the interaction between the spins and their dissipative environment (e.g., spin-phonon coupling constant). Situations with $D/A \gg U/K$ are not impossible.

Therefore, quantitative investigations of relaxation mechanisms based on DM-interactions is of great interest and importance.

VII. SUMMARY

In the present work, we have performed an extensive study of spin excitations in Mn_{12} , explicitly accounting for its many-spin internal structure. The dimerized 8-spin model of the Mn_{12} clusters⁸ has been used. Along with isotropic exchange coupling, various kinds of anisotropic relativistic interactions have been studied: anisotropic exchange coupling between the cluster ions, single-site anisotropies of easy-axis and in-plane type, and various kinds of Dzyaloshinsky-Morya (DM) interactions. Surprisingly, most of these interactions play only a minor role.

As a result, we propose a basic many-spin Hamiltonian which includes isotropic exchange couplings, single-site anisotropies of easy-axis type and DM-interactions between the cluster spins. Three possible sets of parameters are determined from the relevant experimental data. The results of our calculations reproduce satisfactorily various experimental results, such as positions of neutron scattering peaks, high-frequency EPR data and the experimental dependence of the magnetic susceptibility on temperature.

In particular, our results suggest rather strong Dzyaloshinsky-Morya interactions are present in the Mn_{12} cluster. We have discussed qualitatively the possible relation of these interactions to the unusual magnetic relaxational properties of Mn_{12} . We emphasized that DM-interactions present interesting relaxation mechanisms worth further investigations.

ACKNOWLEDGMENTS

Authors would like to thank A. K. Zvezdin, B. Barbara, D. Garanin for many helpful discussions. This work was partially carried out at the Ames Laboratory, which is operated for the U. S. Department of Energy by Iowa State University under Contract No. W-7405-82 and was supported by the Director for Energy Research, Office of Basic Energy Sciences of the U. S. Department of Energy. This work was partially supported by Russian Foundation for Basic Research, grant 98-02-16219.

- ¹ O. Kahn, *Molecular Magnetism* (VCH, New York, 1993); D. Gatteschi, A. Caneschi, L. Pardi and R. Sessoli, *Science* **265**, 1054 (1994).
- ² *Molecular Magnetism: From Molecular Assemblies to the Devices*, ed. by E. Coronado, P. Delhaès, D. Gatteschi and J. S. Miller (Kluwer, Dordrecht, 1996).
- ³ A. J. Leggett, *Suppl. Progr. Theor. Phys.* **69**, 80 (1980).
- ⁴ *Quantum Tunneling of Magnetization — QTM'94*, ed. by L. Gunther and B. Barbara, NATO ASI Ser. E, Vol. 301 (Kluwer, Dordrecht, 1995).
- ⁵ M. B. Menskii *Continuous Quantum Measurements and Path Integrals* (IOP Publishing, Bristol, 1993).
- ⁶ P. W. Shor, *SIAM J. Comput.* **26**, 1484 (1997); N. Gershenfeld and I. L. Chuang, *Science* **275**, 350 (1997).
- ⁷ T. Lis, *Acta Cryst.* **B36**, 2042 (1980); R. Sessoli, D. Gatteschi, A. Caneschi and M. A. Novak, *Nature* **365**, 141 (1993).
- ⁸ R. Sessoli, H.-L. Tsai, A. R. Shake, S. Wang, J. B. Vincent, K. Folting, D. Gatteschi, G. Christou, D. N. Hendrickson, *J. Am. Chem. Soc.* **115**, 1804 (1993).
- ⁹ J. R. Friedman, M. P. Sarachik, J. Tejada and R. Ziolo, *Phys. Rev. Lett.* **76**, 3830 (1996).
- ¹⁰ L. Thomas, F. Lioni, R. Ballou, D. Gatteschi, R. Sessoli and B. Barbara, *Nature* **383**, 145 (1996).
- ¹¹ F. Hartmann-Boutron, P. Politi and J. Villain, *Int. J. Mod. Phys.* **10**, 2577 (1996).
- ¹² B. Barbara, W. Wernsdorfer, L. C. Sampaio, J. G. Park, C. Paulsen, M. A. Novak, R. Ferré, D. Mailly, R. Sessoli, A. Caneschi, K. Hasselbach, A. Benoit, L. Thomas, *J. Magn. Magn. Mater.* **140-144**, 1825 (1995).
- ¹³ C. Paulsen and G. Park, in *Quantum Tunneling of Magnetization* (Ref. 4), p. 189.
- ¹⁴ A. Caneschi, D. Gatteschi, L. Pardi and R. Sessoli, in *Perspectives on Coordination Chemistry*, ed. by A. F. Williams, C. Florani and A. E. Merbach (VCH, Basel, 1992).
- ¹⁵ A. K. Zvezdin and A. I. Popov, *Sov. Phys. JETP* **82**, 1140 (1996).
- ¹⁶ M. Hennion, L. Pardi, I. Mirebeau, E. Suard, R. Sessoli and D. Gatteschi, *Phys. Rev. B* **56**, 8819 (1997).
- ¹⁷ A. M. Gomes, M. A. Novak, R. Sessoli, A. Caneschi and D. Gatteschi, *Phys. Rev. B* **57**, 5021 (1998).
- ¹⁸ B. Barbara, L. Thomas, F. Lioni, A. Sulpice and A. Caneschi, *J. Magn. Magn. Mater.* **177-181**, 1324 (1998).
- ¹⁹ A. A. Mukhin, A. K. Zvezdin, V. V. Platonov, O. M. Tatarsenko, A. Caneschi, D. Gatteschi and B. Barbara, in *Proceedings of ICM'97 Conference*, Cairns, Australia, July 27 – August 1, 1997 (unpublished).
- ²⁰ Although this symmetry is not exact, the deviation from the symmetry is small. Such approximate symmetries are widely used in physics: e.g., the crystal lattice of ferromagnetic iron is often considered as cubic, though actually it is tetragonally distorted.
- ²¹ A. L. Barra, D. Gatteschi and R. Sessoli, *Phys. Rev. B* **56**, 8192 (1997).

- ²² K. Yosida, *Theory of Magnetism* (Springer-Verlag, Berlin, New York, 1996).
- ²³ S. Hill, J. A. A. J. Perenboom, N. S. Dalal, T. Hathaway, T. Stalcup and J. S. Brooks, Phys. Rev. Lett. **80**, 2453 (1998).
- ²⁴ F. Luis, J. Bartolomé, J. F. Fernández, J. Tejada, J. M. Hernández, X. X. Zhang, and R. Ziolo, Phys. Rev. **B 55**, 11 448 (1997).
- ²⁵ See e.g., R. M. White, *Quantum Theory of Magnetism* (Springer-Verlag, Berlin, New York, 1983).
- ²⁶ A. Crépieux and C. Lacroix, J. Magn. Magn. Mater. **182**, 341 (1998).
- ²⁷ V. V. Dobrovitski and A. K. Zvezdin, Europhys. Lett. **38**, 377 (1997); L. Gunther, Europhys. Lett. **39**, 1(1997).
- ²⁸ D. A. Garanin and E. M. Chudnovsky, Phys. Rev. **B 56**, 11 102 (1997).
- ²⁹ A. Fort, A. Rettori, J. Villain, D. Gatteschi and R. Sessoli, Phys. Rev. Lett. **80**, 612 (1998).
- ³⁰ A. L. Burin, N. V. Prokof'ev and P. C. E. Stamp Phys. Rev. Lett. **76**, 3040 (1996).
- ³¹ R. Sessoli, Mol. Cryst. Liq. Cryst. **274**, 145 (1995).

FIG. 1. Schematic plot of the Mn_{12} cluster. Small black circles represent Mn^{4+} ions, large white circles — Mn^{3+} ions. Different types of lines connecting the ions (solid, dashed, dotted and dash-dotted) correspond to different types of exchange interactions (J_1 , J_2 , J_3 and J_4).

FIG. 2. A schematic plot of the 8-spin system representing the Mn_{12} cluster. White large circles represent large spins ($S = 2$), and dark small squares represent small dimer spins ($s = 1/2$).

FIG. 3. Dependence of the normalized cross-section vs. level energy (in K), calculated for the three sets of the cluster parameters (A, B and C, see text). The levels producing noticeable neutron peaks can be easily discriminated from the others.

FIG. 4. Temperature dependence of the effective magnetic moment of the cluster μ_{eff} (in Bohr's magnetons). Results of calculations with the three sets of parameters are shown: the set A (solid line), the set B (dashed line) and the set C (dotted line). Large solid squares represent experimental data. The results of calculations with the sets A and B are very close to each other, and the corresponding curves merge on the figure.

TABLE I. The positions of neutron peaks: comparison between experimental data and calculated results. Calculations have been made for the three possible sets of the cluster parameters (A, B and C, see text). The levels with normalized cross-section more than 0.05 and energy less than 130 K are included in the table.

Experiment	Set A	Set B	Set C
14.4 K	14.4 K	14.4 K	14.4 K

Low-energy peaks (1.2 THz)	57 K	58.2 K	55.2 K	56.7 K
	66 K	66.0 K	66.7 K	67.0 K
	maybe,		67.4 K	67.9 K
	more	76.6 K		75.7 K
High-energy peaks (2 THz)	90 K	124.4 K	98.3 K	88.8 K
	96 K	124.9 K	105.1 K	110.9 K
	105 K	126.4 K	110.4 K	122.1 K
	maybe,	127.1 K	122.1 K	
	more			

TABLE II. Parameters α and β of the easy-axis anisotropy: comparison between experimental data and calculated results. Calculations have been performed for the three possible sets of the cluster parameters (A, B and C, see text).

	Experiment	Set A	Set B	Set C
α (K)	-0.56	-0.63	-0.68	-0.67
β (mK)	-1.11	-0.7	-0.45	-0.49

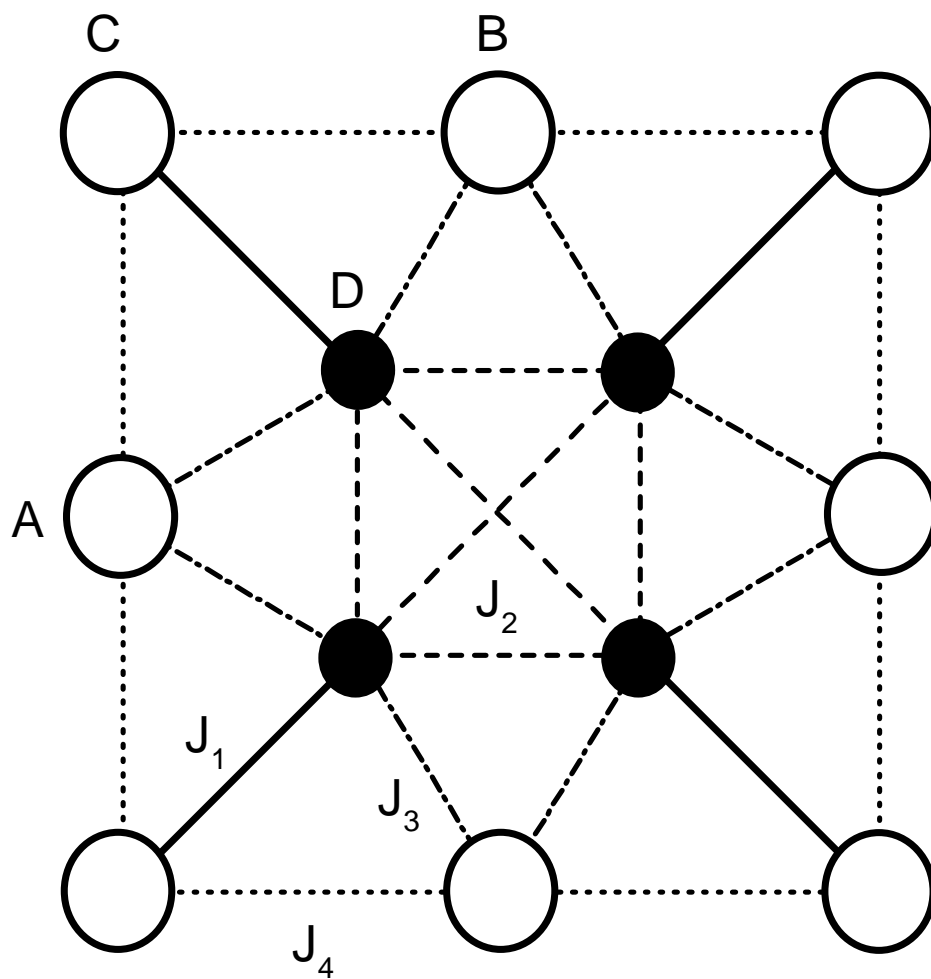


Fig. 1

M.I. Katsnelson "Many-spin interactions ..."

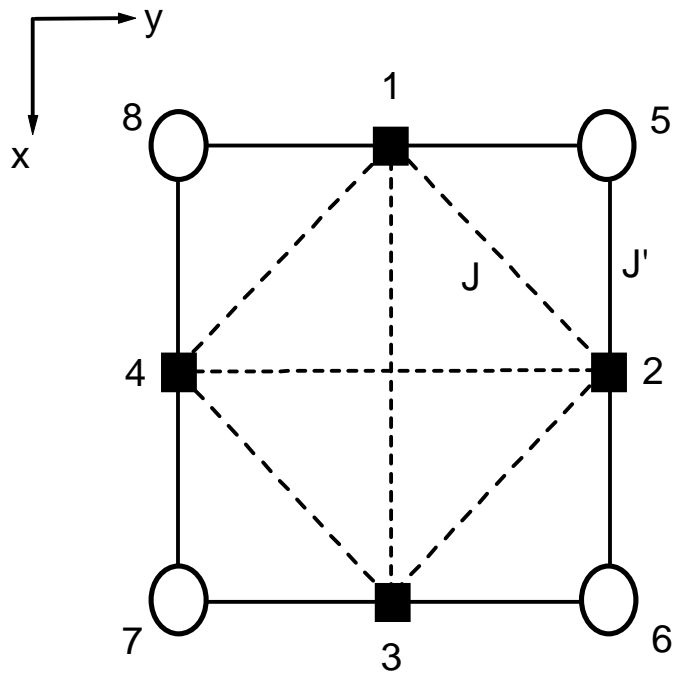


Fig. 2

M.I. Katsnelson "Many-spin interactions ..."

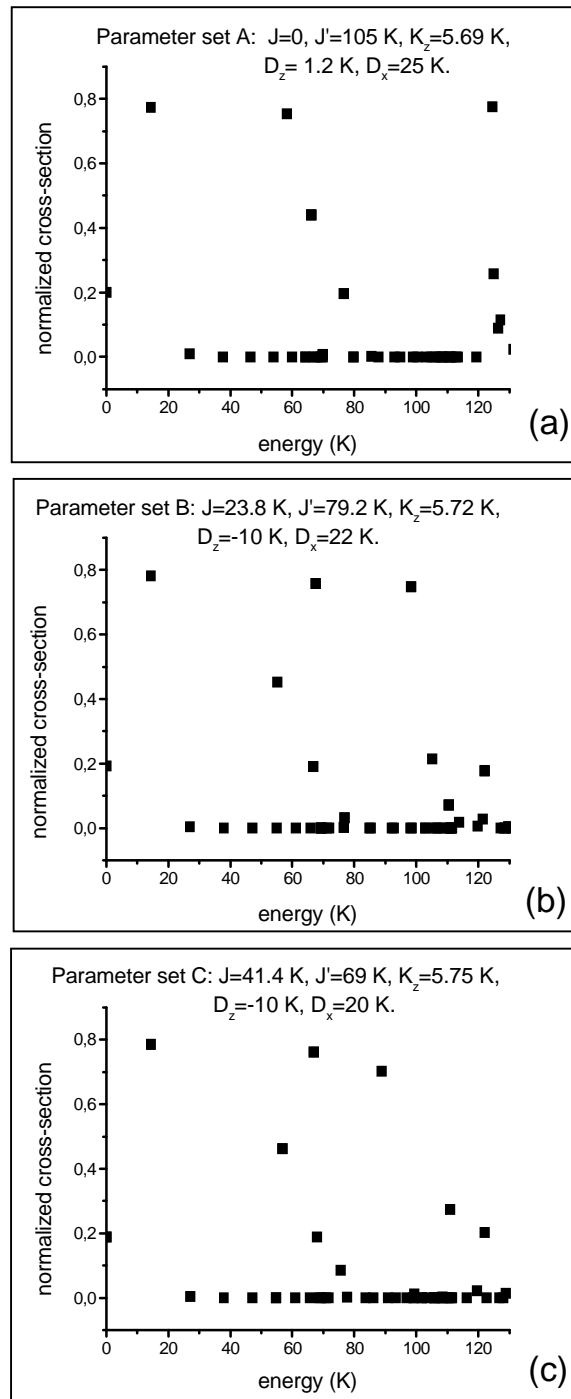


Fig. 3

M.I. Katsnelson et al. "Many-spin interactions..."

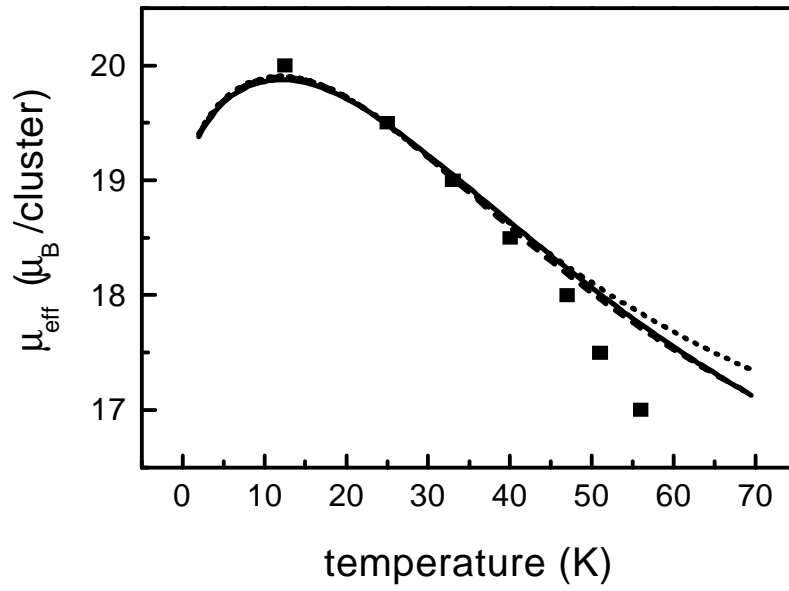


Fig. 4

M.I. Katsnelson "Many-spin interactions ..."